Towards spectrally selective catastrophic response

V. R. Gabriele,[1] A. Shvonski,[1,2] C. S. Hoffman,[3] M. Giersig,[4,5] A. Herczynski,[1] M. J. Naughton,[1] and K. Kempa[1,*]

[1]*Department of Physics, Boston College, Chestnut Hill, Massachusetts 02467, USA*

[2]*Department of Physics, Massachusetts Institute of Technology, Cambridge, Massachusetts 02139, USA*

[3]*Department of Biology, Boston College, Chestnut Hill, Massachusetts 02467, USA*

[4]*Department of Physics, Freie Universität Berlin, 14195 Berlin, Germany*

[5]*International Academy of Optoelectronics at Zhaoqing, South China Normal University, 526238 Guangdong, People's Republic of China*

(Received 26 February 2020; revised manuscript received 22 May 2020; accepted 28 May 2020; published 18 June 2020)

We study the large-amplitude response of classical molecules to electromagnetic radiation, showing the universality of the *transition* from linear to nonlinear response and breakup at sufficiently large amplitudes. We demonstrate that a range of models, from the simple harmonic oscillator to the successful Peyrard-Bishop-Dauxois type models of DNA, which include realistic effects of the environment (including damping and dephasing due to thermal fluctuations), lead to characteristic universal behavior: formation of domains of dissociation in driving force amplitude-frequency space, characterized by the presence of local boundary minima. We demonstrate that by simply following the progression of the resonance maxima in this space, while gradually increasing intensity of the radiation, one must necessarily arrive at one of these minima, i.e., a point where the *ultrahigh spectral selectivity is retained*. We show that this universal property, applicable to other oscillatory systems, is a consequence of the fact that these models belong to the *fold catastrophe* universality class of Thom's catastrophe theory. This in turn implies that for most biostructures, including DNA, high spectral sensitivity near the onset of the denaturation processes can be expected. Such spectrally selective molecular denaturation could find important applications in biology and medicine.

DOI: 10.1103/PhysRevE.101.062415

I. INTRODUCTION

It is well known that molecules can be driven to dissociation by the application of *ionizing radiation*, photons which carry energy sufficient to break molecular bonds. In that class, x rays have long been applied to treat cancer [1]. However, such therapy has little or no spectral resolution, i.e., regardless of the x-ray frequency, all irradiated molecules (at the tumor and/or in the background) are damaged. Resolution therefore must rely on geometric targeting, and thus the treatment is effective only if applied to large tumors. *Nonionizing radiation*, with photon energies in the range well below the covalent bonding energy, can at sufficient field intensity also cause dissociation via nonlinear effects, with demonstrated microgeometrical resolution. For example, microtargeted dissociation of cells using laser tweezers was recently demonstrated [2]. In that experiment, 90% of targeted yeast cells were killed by a low-power (80 mW) near-infrared laser, focused to a spot of about 1 μm diameter. Also, there have been reports of nonthermal effects caused by nonionizing THz radiation, yielding partial dissociation of DNA ("bubble" formation) and affecting gene expression [3,4]. Most importantly, however, nonionizing radiation could allow for spectral resolution of the dissociation.

Such a possibility is suggested already in the simplest harmonic model of a radiation-driven molecule (or its segment), considered as a mass m oscillating due to the action of a spring (of stiffness k) representing the molecular bond, with y representing the bond length. In this textbook model [5], the dynamics of the oscillatory motion are readily obtained using the standard analysis of a damped oscillator, driven by force $F(t) = F_0 \sin(\omega t)$, with frequency ω and time t. The dissociation of the molecule in this case can be defined as a state with amplitude of oscillations $\bar{y}$ exceeding a critical amplitude $y_{\max}$ for molecular breakup (dissociation). The required force amplitude for this to occur is given by

$$F_0 = \beta\left[\left(\frac{\Delta\omega}{\omega_0}\right)^2 + \left(\frac{\gamma}{\omega_0}\right)^2\right]^{1/2}, \tag{1}$$

where $\gamma \ll \omega_0$ is the damping index, $\Delta\omega = \omega - \omega_0$, ($|\Delta\omega| \ll \omega_0$, with $\omega_0 = \sqrt{k/m}$), and $\beta = 2y_{\max}\, m\omega_0^2$. Figure 1(a) shows the amplitude-frequency space (AFS) plot for this model, i.e., F_0 vs ω, as in Eq. (1). Clearly, the domain of dissociation has a quasiparabolic boundary, with a well-defined minimum at $\omega = \omega_0$. This result, obtained under the simplifying assumption of *linear* response, implies excellent spectral sensitivity of the dissociation transition, since at $F_0/\beta = \gamma/\omega_0$, the structure is stable for any $\omega \neq \omega_0$, and dissociates only for $\omega = \omega_0$. Also, it is important to note that in the stable domain of AFS, $\bar{y}$ has a single maximum at the resonance frequency, which in this very simple model, and for all driving amplitudes, is just ω_0. Thus, the corresponding "trace" of these maxima in AFS is simply a vertical line at

*kempa@bc.edu

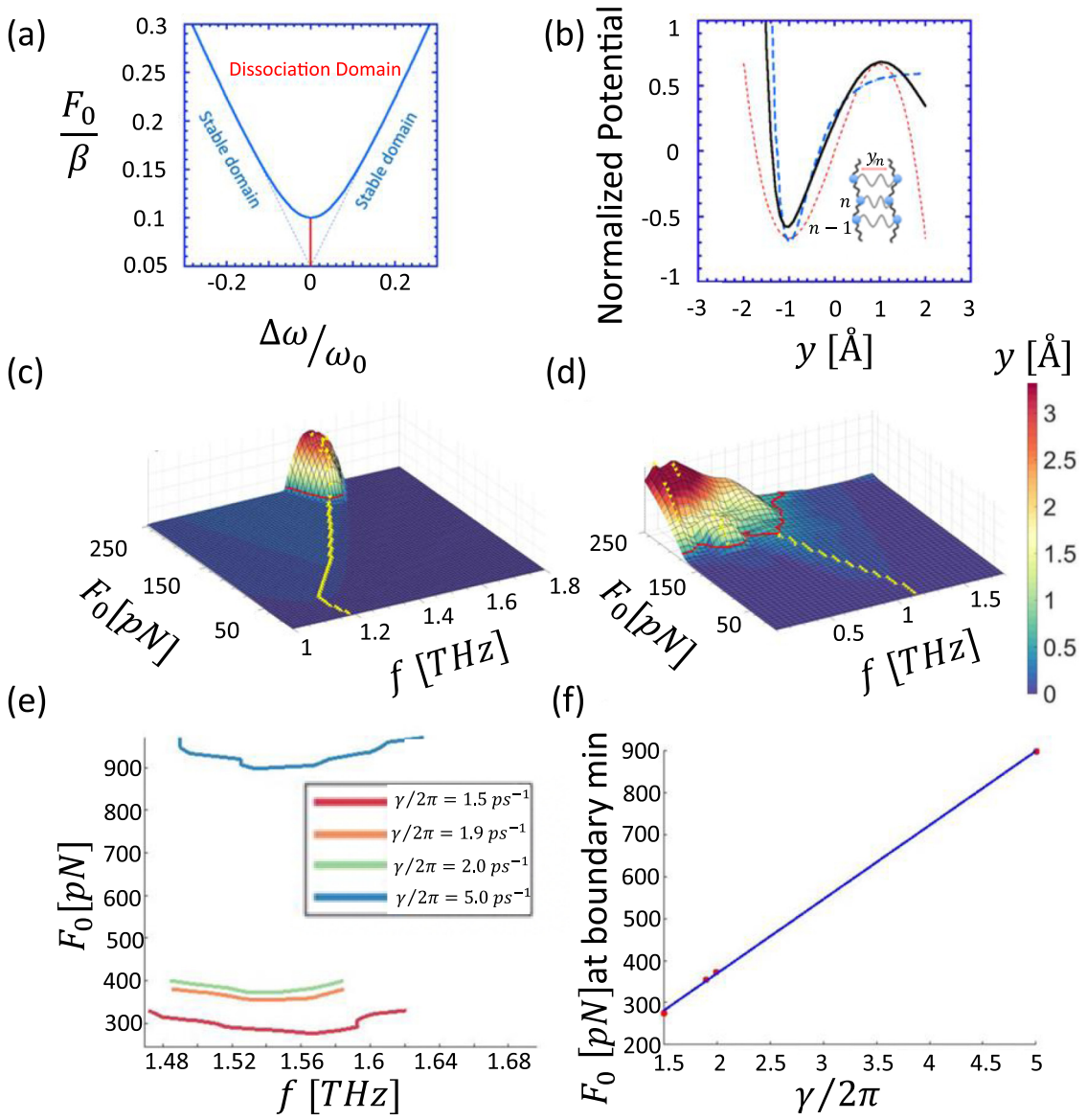

FIG. 1. (a) AFS for the simple harmonic model of a molecule, with $\gamma/\omega_0 = 0.1$. (b) Normalized total equilibrium potentials vs y, from the fold catastrophe universality class: red-dotted line [Eq. (2)], bold-solid line [Eq. (4), modified Morse], dashed-blue line [Eq. (4) with $G_n = 0$, Morse]. Inset shows a model of the DNA fragment. (c) 3D map of the amplitude-frequency-displacement response of the DNA (poly-AT BP at $T = 1$ K), simulated using the modified Morse potential [Eq. (4)]. (d) 3D map of the amplitude-frequency-displacement response of the DNA, simulated using the Morse potential [Eq. (4) with $G_n = 0$] at $T = 1$ K. In both (c) and (d), $\gamma/2\pi = 1$ ps^{-1}. (e) Dissociation boundaries near $f_{\min}$ for increasing γ. (f) F_0 at the boundary minimum for increasing γ: red dots represent calculations, and the blue straight line is a guide to the eye.

$\omega = \omega_0$, terminating at the bottom of the dissociation domain [red line in Fig. 1(a)].

In the present work, we demonstrate that these main features of dissociation dynamics of the simple harmonic model remain valid in the response of real (in general, nonlinear) large molecules. We do not address the details of the chaotic dynamics that develops near the dissociation domain boundary, but instead focus on the *universality* of dissociation conditions. This includes the fact that the trace of a resonance in the stable domain of AFS connects to the *minimum* of the corresponding dissociation domain boundary, which implies *high spectral resolution* of the dissociation near this minimum, a fact of potential importance for applications.

II. GENERAL CONSIDERATIONS OF MOLECULAR DISSOCIATION

We begin with the most general aspects of molecular dissociation. Consider a molecule large enough so that its dynamics are classical, subject to an interaction potential $U(y)$, where y can be understood as a generalized molecule size (e.g., molecular bond length). We assume this potential to have the following properties: (i) it has a single minimum at $y = y_{\min}$, (ii) for decreasing $y < y_{\min}$ it monotonically increases, and (iii) it has a single maximum at $y = y_{\max} > y_{\min}$. All potentials shown in Fig. 1(b) satisfy these conditions. Consider now the response of this molecule to an oscillatory force as before:

$F(t) = F_0 \sin(\omega t)$. Based on general physical expectation of stronger response to stronger driving (valid in the nonchaotic regime), we make the following key assumption: the maximum (or properly defined time average) of y,$\bar{y} = \mathcal{R}(\omega; F_0)$ *is a monotonically increasing function of* F_0. We show further that this assumption is valid for all models shown in Fig. 1(b). Consequently, the dissociation condition defined by $\bar{y} > y_{\max}$ corresponds to a distinct dissociation domain in the AFS.

As for the simple harmonic oscillator model, we note that $\bar{y} = \mathcal{R}(\omega; F_0)$ must have a maximum due to resonance conditions of the oscillatory motion for $y < y_{\max}$ for any value of the parameter F_0. Its location follows a specific line in the AFS (the trace) from the simple harmonic resonance at $\omega = \omega_0$, corresponding to the necessarily parabolic form of $U(y)$ near the minimum $y = y_{\min}$, to the crossing point into the corresponding dissociation domain at $\omega = \omega_{\rm dis}$. Moreover, if one defines the dissociation domain boundary in the AFS as $F_0 = \mathcal{R}^{-1}(\omega, \bar{y} = y_{\max})$ [6], the point on this boundary at $F_0 = \mathcal{R}^{-1}(\omega_{\rm dis}, \bar{y} = y_{\max})$ is necessarily its *minimum*. This follows immediately from the fact that at the crossing point of the trace with the boundary, the frequency along the boundary departs from the resonance condition, implying that the corresponding amplitude $\bar{y}' < y_{\max}$. This would mean it returns to the oscillatory motion condition (back to the stable domain). In order to stay on the dissociation domain boundary, F_0 must necessarily increase, leading to a larger maximum displacement $\bar{y} > \bar{y}'$, such that again $\bar{y} = y_{\max}$. Thus, $F_0 = \mathcal{R}^{-1}(\omega_{\rm dis}, \bar{y} = y_{\max})$ must be a minimum in the AFS. As will be shown further below, these features are fully confirmed not only by the introductory simple harmonic model, but also by all of the model potentials of Fig. 1(b), including extensions to finite temperatures, multiple potential minima, and molecule-molecule interactions.

The generality of our analysis stems from the fact that $U(y)$ as defined above belongs to the class of potentials with "escape," that lead to the *fold catastrophes* of the catastrophe theory of Thom [7]. Thus, all potentials shown in Fig. 1(b) also belong to this universality class, and consequently share the quasitopological properties of the AFS discussed above. The generic potential functional form in this universality class is given parametrically as [8]

$$U(y) = B\left(-\frac{y^3}{3} + Ay\right). \tag{2}$$

This universal potential, shown as a thin dashed line in Fig. 1(b), can describe catastrophic dynamics of an entire class of physical systems, ranging from a ship subject to rolling motion, which can capsize if it leans too much away from its vertical position [8], to an oscillating molecule, which breaks apart when its bond is stretched beyond a critical length. It was demonstrated in Ref. [8] that y at the dissociation domain boundaries in this class of potentials develops chaotic dynamics, leading to its fingerlike roughness. This effect increases with increasing $y_{\max}$, and in the special case of the Morse potential [shown as blue-dashed line in Fig. 1(b), and for which $y_{max} \to \infty$], the resulting dissociation domain in the AFS has a boundary with multiple minima, connecting to multiple stable modes due to nonlinearities. Detailed analyses of all these models are given below.

III. DISSOCIATION DYNAMICS OF REALISTIC MODELS: MODELING OF DNA

In this section, we confirm by simulations that the analysis of general features of the dissociation dynamics in the AFS remain valid in realistic models of large molecules, with potentials from the fold catastrophe class. There is a family of successful, realistic models of DNA, based on the Peyrard-Bishop-Dauxois (PBD) model [9–18]. Here we chose a PBD model from this family, proposed by Tapia-Rojo, *et al.* [18]. The model describes forces between DNA base pairs (BPs) using a ladderlike geometry [see the inset in Fig. 1(b)]. The dynamics are parametrized by the coordinate $y_{\rm n}$, which is defined as the normalized separation between nucleotides in the nth BP. These coordinates are normalized relative to their equilibrium position (at $T = 0$), which is $y_{\rm n} = 0$ in a center of mass frame of the BP. The equation of motion (Newton's second law) is

$$\begin{aligned} m\ddot{y}_n = & -U'(y_n) - W'(y_n,\ y_{n+1}) - W'(y_n,\ y_{n-1}) \\ & - m\gamma\dot{y}_n - \eta(t) - F(t), \end{aligned} \tag{3}$$

where $\dot{y}_n = \frac{\partial}{\partial t} y_n$, $\ddot{y}_n = \frac{\partial^2}{\partial^2 t} y_n$, and the primed terms are defined by $\phi' = \frac{\partial}{\partial y_{\rm n}}\phi$. The external driving force is again $F(t) = F_0 \sin(\omega t)$. Thermal fluctuations are realistically accounted for (in real time) using the Langevin forcing term $\eta(t)$, which represents a random force drawn from a thermal Gaussian distribution with variance $2m\gamma k_B T$ [18]. These thermal fluctuations, as well as the homogeneous damping due to the environment (the velocity term, scaled by parameter γ) are important, and their inclusion is crucial in achieving agreement with experiment. The interaction within the nth BP is governed by a modified Morse intrabase pair potential given by

$$U(y_n) = D_n[\exp(-\alpha_n y_n) - 1]^2 + G_n \exp[-(y_n - d_n)^2/b_n]. \tag{4}$$

Figure 1(b) shows plots of scaled $U(y_n)$, in a shifted reference frame, for the case of nonzero G_n (bold black line), and for $G_n = 0$ (Morse potential, dashed blue line). The outer phosphate backbone provides an effective interbase pair potential $W(y_n, y_{n\pm1})$, the so-called 'stacking" potential:

$$W(y_n,\ y_{n\pm1}) = \frac{k}{2}\{1 + \rho \exp[-\delta(y_n + y_{n\pm1})](y_n - y_{n\pm1})^2\}. \tag{5}$$

To solve Eq. (3), we used a Verlet-type algorithm [19] for a sequence of $N = 64$ BPs, with periodic boundary conditions. The parameters D_n, α_n, G_n, d_n, and b_n are BP specific; all others are independent of BP type, and were taken from Ref. [18]. Specific values of all parameters employed are $D_n[\mathrm{AT}] = 0.05185\,\mathrm{eV}$, $\alpha_n[\mathrm{AT}] = 4\,\mathrm{\AA}^{-1}$, $D_n[\mathrm{GC}] = 1.5\,D_n[\mathrm{AT}]$, $\alpha_n[\mathrm{GC}] = 1.5\alpha_n[\mathrm{AT}]$, $G_n = 3D_n$, $d_n = 2/\alpha_n$, $b_n = 1/(2\,\alpha_n^2)$, $k = 0.03\ \mathrm{eV\,\mathrm{\AA}^{-2}}$, $\rho = 3$, $\delta = 0.8\,\mathrm{\AA}^{-1}$, $\gamma/2\pi = 1\ \mathrm{ps}^{-1}$, and $m = 300$ amu.

For $F(t) = 0$ and after achieving equilibration at $T = 290\,\mathrm{K}$, the results for a homogeneous sequence of AT base pairs were fully consistent with those reported in Ref. [20]. In particular, random "bubbles" [local DNA unzippinglike

dissociation (denaturation)] appeared in a temperature range just below the melting temperature of $T = 314$ K, and above this temperature a complete denaturation of DNA, i.e., full separation of the strands, followed. For $F_0 \neq 0$, the behavior of the DNA model for different driving amplitudes F_0 and frequencies $\omega = 2\pi f$ was simulated to determine regions of dissociation (denaturation), and the traces of the corresponding resonances in the AFS. Figures 1(c) and 1(d) show 3D maps of the amplitude-frequency-displacement response of the DNA at a very low temperature of $T = 1$ K, and using the modified Morse potential [using full Eq. (4)] and the Morse potential of Eq. (4) with $G_n = 0$ (no Gaussian barrier), respectively. We begin with this very low temperature in order to suppress thermal fluctuations, and thus to assess their relative importance as compared to homogeneous damping. As expected, in this low-T case, homogeneous damping is dominant: the oscillations spectrum is well defined (coherent) but strongly damped, since the experimentally determined damping parameter is large: $\gamma/2\pi = 1$ ps^{-1}. This results in a very small quality factor of $Q = \omega_0/\gamma \approx 1$ for the main resonance. Displacement of the nth BP is defined here as $\bar{y}_n = \sqrt{\langle y_n^2 \rangle}$, where $\langle\ \rangle$ symbolizes a simple time average over one driving force period.

The AFS is simply given by a cross-sectional cut through a given map, with a horizontal plane at corresponding $\bar{y}_n = y_{\max}$. The dissociation domain boundary is marked with a red line, and the trace of the resonances as yellow dots. It is clear from Fig. 1 that the topology of the AFS for the DNA-models is the same as for the simple harmonic model [Fig. 1(a)]. In all cases, there is a well-defined minimum of the single dissociation domain boundary at $f_{\min}$, at the crossing point with the resonance trace, which implies sharp spectral selectivity. Specifically, for the modified Morse model [Eq. (4), with nonzero G_n], the boundary of the dissociation domain is quasiparabolic, and the resonance trace is initially slightly redshifted, but then blueshifts for $F_0 > 50$ pN, until it arrives at the frequency $f_{\min} = 1.52$ THz. For the pure Morse model [$G_n = 0$ in Eq. (4)], the shape of the dissociation domain is irregular and asymmetric (in full agreement with an earlier study of chaotic behavior of the model [21]), and the frequency trace is redshifted throughout the range (as required [22]), reaching the still well-defined local minimum of the dissociation domain boundary at $f_{\min} = 0.8$ THz. Note that at low temperatures [i.e., when $\eta(t) \to 0$], the stacking potential $W(y_n,\ y_{n\pm1})$ given by Eq. (4) can be assumed zero, since the driving force is long wavelengths (depends only on frequency), which immediately implies that $y_1 = y_2 = \ldots = y_n = \ldots y_N$, leading to $W(y_n,\ y_{n\pm1}) = 0$, for all n. We have confirmed this by simulations: for $T = 1$ K the traces indeed remain essentially unchanged by setting $W(y_n,\ y_{n\pm1}) = 0$, except very close to (and of course in) the dissociation domains. We have also shown that in almost the entire trace range $\bar{y}_n = \sqrt{\langle y_n^2 \rangle} \approx B\langle y_n \rangle$, where $B > 0$ is a scaling constant. This shows that it is the confining potential asymmetry which is the dominant part of the nonlinear behavior that controls the trace dynamics at low temperatures. Note that for a completely symmetric potential (linear or not), the time average $\langle y_n \rangle = 0$. We have also confirmed that the topology of AFS survives much larger damping. Figure 1(e) shows dissociation boundaries near $f_{\min}$ for various γ, well defined even for $\gamma/2\pi = 5$ ps^{-1} ($Q \ll 1$). The main effect of increasing γ is the upward shift of the dissociation domain. This is expected, since larger driving amplitudes are needed to overcome the increased damping. Figure 1(f) shows that F_0 at the boundary minima is proportional to γ, exactly as the simple harmonic model predicts [see Eq. (1), for $(\frac{\Delta\omega}{\omega_0}) \to 0$].

The topology of the DNA models also survives dephasing thermal fluctuations at room temperatures ($T = 290$ K), which dominate the low-amplitude F_0 physics. This is demonstrated in Fig. 2(a), which shows the AFS for the modified Morse potential [Eq. (4)] with nonzero stacking potential [Eq. (5)], simulated for DNA with AT BPs. Figure 2(b) shows the same for DNA with GC BPs. The corresponding $\bar{y}_n$ is color coded, and clearly shows the dissociation domains, with well-defined boundaries (red line). In both cases, the yellow points, which represent local resonance maxima of a single nth BP, are randomly scattered in the entire range of frequencies displayed, for this very small F_0. The random scatter means the absence of a well-defined resonance frequency, as a result of the fluctuation dephasing. Note that in the case of very low temperatures (e.g. 1 K) shown in Figs. 1(c) and 1(d), the scatter of the yellow points is not visible due to vanishingly small thermal dephasing. Most importantly, the increasing driving force restores coherence of the resonances, which is visible as narrowing of the scatter ranges in Figs. 2(a) and 2(b). This is a well-known effect in the theory of instabilities or lasing: the driving force compensates for losses, and at this point the system acquires gain, and becomes unstable (in our case it enters the dissociation domain).

If the details of the fluctuation dynamics were not needed, one could average out these fluctuations over all of the 64 BP locations. The result would be a flat spectrum in the scatter range. Further simplification, often used in response calculations (e.g,. RPA, for not too high temperatures) is to include this effect (effectively) as additional homogeneous damping (e.g., by simply changing γ into $\gamma' > \gamma$). The quantum-mechanical justification of this approach is that the averaged damping in a system of charges results from scattering events between these charges and the environment (homogeneous) and phonons (thermal dephasing). Additivity of these two scattering processes in the response functions has been demonstrated [23]. We do not make such assumptions here, but in the spirit of this approach we could interpret the trace scatter as corresponding to a large effective thermal damping, which for very small F_0 leads to a vanishingly small $Q \ll 1$. On the other hand, for large F_0, the scatter range narrows, as discussed above, which could also be viewed as lowering of the overall damping, and thus dramatically increasing Q.

Occurrence of the dissociation domains in different areas of the AFS could allow also for selective dissociation of specific segments of DNA. For example, Figs. 2(a) and 2(b) indicate that driving a DNA molecule with $F_0 = 150$ pN and $f = \frac{\omega}{2\pi} = 1.45$ THz would dissociate only the AT BPs, leaving the GC BPs unaffected. Conversely, for $F_0 = 250$ pN and $f = \frac{\omega}{2\pi} = 2.8$ THz, only GC BPs would be dissociated. This potentially fine control of the segment dissociation (creation of localized bubbles) is further demonstrated in Figs. 2(c) and 2(d). The left panel shows the AT BP sequence with a single GC BP inclusion, driven by external force with

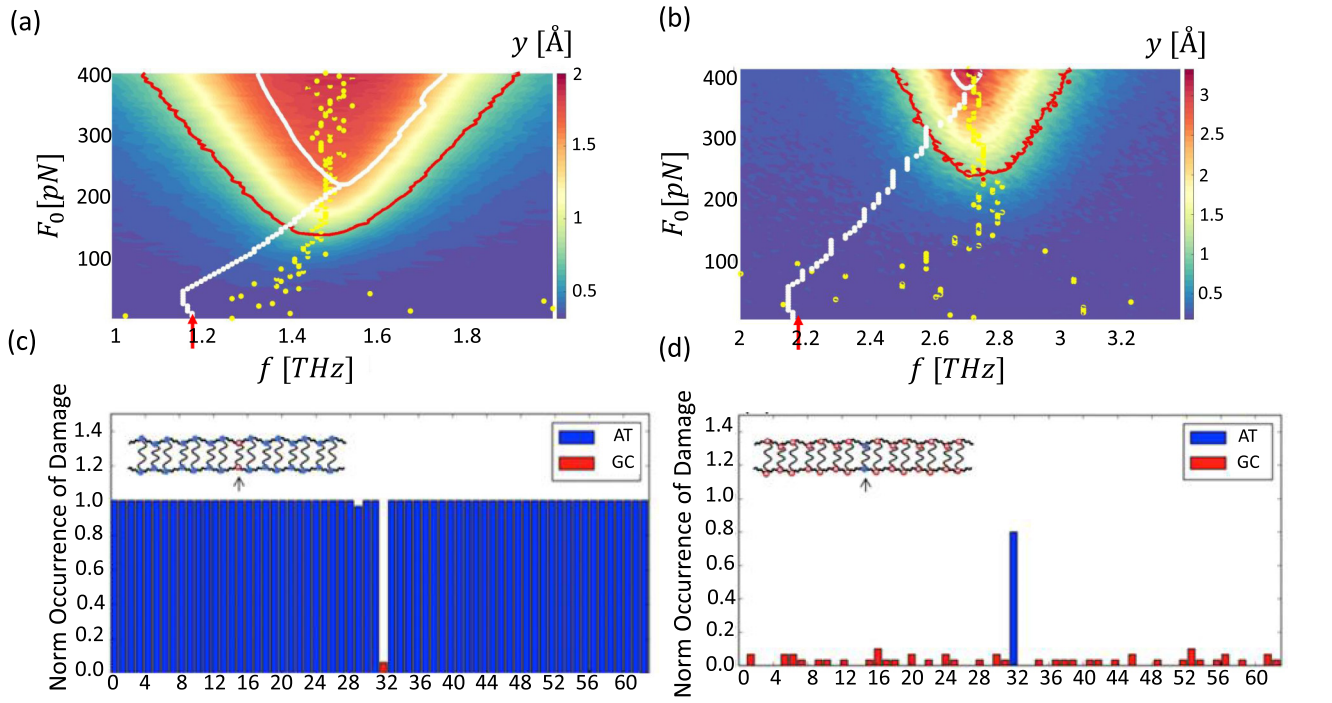

FIG. 2. (a), (b) Color maps of the DNA dynamics, showing an average (color-encoded) separation y_n of the BP [AT for (a), and GC for (b)], vs driving parameters F_0 and $f = \omega/2\pi$, at $T = 290$ K. The red line in each figure represents the corresponding dissociation boundary curve. The critical BP separation for denaturation $y_{\max}$ is 0.5125 Å in (a), and 0.338 Å in (b). The red arrows represent the corresponding linear resonance frequencies ($f_0 = 1.26$ THz for AT BPO, and $f_0 = 2.21$ THz for GC BP). Yellow dots indicate the resonance maxima locations. White dots show the resonance maxima locations and the dissociation boundary at $T = 1$ K. (c), (d) Histograms of normalized number of occurrences of damage (in over 30 independent trials), when only the AT BP exceeds its denaturation threshold. This result is fully consistent with AFS maps in Figs. 1(c) and 1(d).

$F_0 = 400$ pN and $f = \frac{\omega}{2\pi} = 1.5$ THz. According to Figs. 2(a) and 2(b), this condition places the system in the region of certain dissociation for AT BPs, and stability for GC BPs, and Figs. 2(c) and 2(d) indicate this as well. Under the same driving conditions, and for the GC BP sequence with an AT BP inclusion, only this AT BP inclusion would be dissociated, again in agreement with Figs. 2(a) and 2(b). This conclusion remains the same for a variety of different BP combinations and numbers.

Finally, it should be noted that it is possible to drive the system with a more complicated, nonsinusoidal excitation. This approach is discussed in Ref. [24], and more recently it was demonstrated that complex molecules ^{7}Li ^{35}Cl and ^{7}Li ^{37}Cl can be selectively dissociated with properly engineered trains of terahertz pulses [25]. The problem of dissociation with nonsinusoidal excitations is nontrivial, in general, due to nonlinearity of the response; the simple additivity of the response to a sum of the Fourier components of complex excitations is no longer valid.

IV. CONCLUSIONS

We have studied large classical molecules from the fold catastrophe universality class of catastrophe theory, focusing on universality of the *transition* from linear behavior at low amplitudes, to dissociation at sufficiently large amplitudes. We show that for a range of models from this class, from the simple harmonic oscillator to the successful, realistic PBD-type models of DNA, the amplitude-frequency space of the driving force has the same topology: dissociation domains with local, dissociation domain boundary minima. We demonstrate that by simply following the progression of a linear resonance maximum, while increasing gradually the intensity of the radiation, one must necessarily arrive at one of these minima, i.e., a point where *high spectral selectivity is retained*. We show that this universal property is a consequence of the fact that these models belong to the fold catastrophe universality class of Thom's catastrophe theory. This implies that for such molecules, including DNA, a high spectral sensitivity near the onset of the denaturation processes can be expected.

The universality of the basic topological structure of the AFS domains implies high spectral and dynamical resolution of the large-amplitude dynamics of the structures, including dissociation, which could lead to various applications. For example, one might be able to target and irreversibly damage, *in vivo*, foreign or mutated biomolecules or cells, provided that the driving radiation can sufficiently penetrate the target medium, and the domains of dissociation do not strongly overlap. Such precise, ultrafast molecular dissociation engineering could lead to highly effective medical treatments and therapies. Note that this strategy would be preferable to existing "Trojan horse" therapies (e.g., photothermal), which deploy particle (including nanoparticle) species chemically bound to the biological targets, and subsequently activated (e.g., overheated) by external radiation. Therapies based on

the dissociation engineering proposed here could be used to treat viral and bacterial infections. This could be particularly beneficial, given a steady rise of microorganisms resistant to antibiotics in this "postantibiotic era" [26]. These therapies might also be used to address disorders involving mutated DNA, or prion diseases involving misfolded proteins [27]. Similarly, amyloidosis and neurodegenerative diseases such as Alzheimer's disease are associated with the presence of amyloid proteins and other protein aggregations [28] and could be treated in the same way. Finally, this method could also prove effective in destroying cancerous cells, particularly in the most deadly, metastatic phase.

ACKNOWLEDGMENTS

This work was supported by National Science Foundation Grant No. 1748906. M.G. acknowledges support by the Guangdong Innovative and Entrepreneurial Team Program (No. 2016ZT06C517).

[1] R. Baskar, K. A. Lee, R. Yeo, and K. W. Yeoh, Cancer and radiation therapy: Current advances and future directions, Int. J. Med. Sci. **9**, 193 (2002).

[2] Z. Pilát, A. Jonáš, J. Ježek, and P. Zemánek, Effects of infrared optical trapping on *Saccharomyces cerevisiae* in a microfluidic system, Sensors **17**, 2640 (2017).

[3] K. T. Kim, J. Park, S. J. Jo, S. Jung, O. S. Kwon, G. P. Gallerano, W-Y. Park, and G-S. Park, High-power femtosecond-terahertz pulse induces a wound response in mouse skin, Nat. Sci. Rep. **3**, 2296 (2013).

[4] M. Gonzales-Jimenez, G. Ramakrishnan, T. Harwood, A. J. Lapthorn, S. M. Kelly, E. M. Ellis, and K. Wynne, Observation of coherent delocalized phonon-like modes in DNA under physiological conditions, Nat. Commun. **7**, 11799 (2016).

[5] K. R. Symon, *Mechanics* (Addison-Wesley, Reading, MA, 1971).

[6] Existence of the inverse is assured on physical grounds.

[7] R. Thom and V. I. Arnold, *Catastrophe Theory*, 3rd ed. (Springer-Verlag, Berlin, 1992).

[8] A. Y. Kuznetsova, A. P. Kuznetsov, C. Knudsen, and E. Mosekilde, Catastrophe theoretic classification of nonlinear oscillators, Int. J. Bifurc. Chaos **14**, 1241 (2004).

[9] M. Peyrard and A. R. Bishop, Statistical Mechanics of a Nonlinear Model for DNA Denaturation, Phys. Rev. Lett. **62**, 2755 (1989); B. S. Alexandrov, N. K. Voulgarakis, K. Ø. Rasmussen, A. Usheva and A. R. Bishop, Pre-melting dynamics of DNA and its relation to specific functions, J. Phys.: Condens. Matter **21**, 034107 (2009); B. S. Alexandrov, V. Gelev, Y. Monisova, L. B. Alexandrov, A. R. Bishop, K. Ø. Rasmussen, and A. Usheva, A nonlinear dynamic model of DNA with a sequence-dependent stacking term, Nucleic Acids Res. **37**, 2405 (2009).

[10] G. Kalosakas, K. Ø. Rasmussen, and A. R. Bishop, Charge trapping in DNA due to intrinsic vibrational hot spots, J. Chem. Phys. **118**, 3731 (2003).

[11] C. H. Choi, G. Kalosakas, K. O. Rasmussen, M. Hiromura, A. R. Bishop, and A. Usheva, DNA dynamically directs its own transcription initiation, Nucl. Acid. Res. **32**, 1584 (2004).

[12] K. B. Blagoev, B. S. Alexandrov, E. H. Goodwin, and A. R. Bishop, Ultra-violet light induced changes in DNA dynamics may enhance TT-dimer recognition, DNA Repair **5**, 863 (2006).

[13] N. K. Voulgarakis, A. Redondo, A. R. Bishop, and K. Ø. Rasmussen, Probing the Mechanical Unzipping of DNA, Phys. Rev. Lett. **96**, 248101 (2006).

[14] L. B. Alexandrov, K. Ø. Rasmussen, A. R. Bishop, and B. S. Alexandrov, Evaluating the role of coherent delocalized phonon-like modes in DNA cyclization, Nat. Sci. Rep. **7**, 9731 (2017).

[15] A. E. Bergues-Pupo, J .M. Bergues, and F. Falo, Modeling the interaction of DNA with alternating fields, Phys. Rev. E **87**, 022703 (2013).

[16] A. E. Bergues-Pupo, J. M. Bergues, and F. Falo, Unzipping of DNA under the influence of external fields, Physica A **396**, 99 (2014).

[17] T. Dauxois, M. Peyrard, and A. R. Bishop, Entropy-driven DNA denaturation, Phys. Rev. E **47**, R44 (1993).

[18] R. Tapia-Rojo, J. J. Mazo, and F. Falo, Thermal and mechanical properties of a DNA model with solvation barrier, Phys. Rev. E **82**, 031916 (2010).

[19] N. Grønbech-Jensen and O. Farago, A simple and effective Verlet-type algorithm for simulating Langevin dynamics, Mol. Phys. **111**, 983 (2013).

[20] E. S. Swanson, Modeling DNA response to terahertz radiation, Phys. Rev. E **83**, 040901(R) (2011).

[21] G. C. Lee and J.-M. Yuan, Bistable and chaotic behaviour in a damped driven Morse oscillator: A classical approach, J. Chem. Phys. **84**, 5486 (1986).

[22] N. B. Slater, Classical motion under a Morse potential, Nature (London) **180**, 1352 (1957).

[23] R. D. Mattuck, *A Guide to Feynman Diagrams in the Many-Body Problem*, 2nd ed. (McGraw-Hill, New York, 1976).

[24] A. Hubler and E. Luscher, Towards spectrally selective catastrophic response, Naturwissenschaften **76**, 67 (1989).

[25] A. Ichihara, L. Matsuoka, E. Segawa, and K. Yokoyama, Isotope-selective dissociation of diatomic molecules by terahertz optical pulses, Phys. Rev. A **91**, 043404 (2015).

[26] K. Lewis, Platforms for antibiotic discovery, Nat. Rev. Drug Discov. **12**, 371 (2013); D. G. Murphy and J. P. Grummet, Planning for the post-antibiotic era - Why we must avoid TRUS-guided biopsy sampling, Nat. Rev. Urol. **13**, 559 (2016).

[27] A. Annus, A. Csati, and L. Vecsei, Prion diseases: New considerations, Clin. Neurol. Neurosurg. **150**, 125 (2016).

[28] M. Goedert, M. Masuda-Suzukake, and B. Falcon, Like prions: the propagation of aggregated tau and α-synuclein in neurodegeneration, Brain **140**, 266 (2017).